

Cardiac repolarization: Insights from mathematical modeling and electrocardiographic imaging (ECGI)

Yoram Rudy, PhD, FAHA, FHRS

From the Cardiac Bioelectricity and Arrhythmia Center, Washington University in St. Louis, St. Louis, Missouri.

Cardiac repolarization is a complex rate dependent process. At the cellular level, it depends on a delicate dynamic balance of ion channel currents. At the heart level, it is spatially heterogeneous, leading to spatial gradients of potential and excitability.

This article provides insights into the molecular mechanisms of the delayed rectifiers I_{Kr} (rapid) and I_{Ks} (slow) that underlie effective function of these channels as repolarizing currents during the cardiac action potential (AP). We also provide non-invasive images of cardiac repolarization in humans. Methodologically, computational biology is used to simulate ion channel function and to incorporate it into a model of the cardiac cell. ECG imaging (ECGI) is applied to normal subjects and Wolff-Parkinson-White (WPW) patients to obtain epicardial maps of repolarization. The simulations demonstrate that I_{Kr} and I_{Ks} generate their peak current late during the AP, where they effectively participate in repolarization. I_{Kr} maximizes the current by fast inactivation and gradual recovery during the AP. I_{Ks} does so by generating an available reserve of channels in closed states from which the channels can open rapidly. ECGI

shows that in the human heart, normal repolarization epicardial potential maps are static with 40 ms dispersion between RV and LV. In WPW, ECGI located the accessory pathway(s) and showed a large base-to-apex repolarization gradient that resolved to normal one month post-ablation, demonstrating presence of "cardiac memory". We conclude that computational biology can provide a mechanistic link across scales, from the molecular functioning of ion channels to the cellular AP. ECGI can non-invasively image human cardiac repolarization and its alteration by disease and interventions. This property makes it a potential tool for noninvasive risk stratification and evaluation of treatment by drugs and devices.

KEYWORDS Cardiac repolarization; Ion channels; Imaging; WPW

ABBREVIATIONS AP = action potential; ECGI = electrocardiograph imaging; WPW = Wolff-Parkinson-White

(Heart Rhythm 2009;6:S49–S55) © 2009 Published by Elsevier Inc. on behalf of Heart Rhythm Society.

Introduction

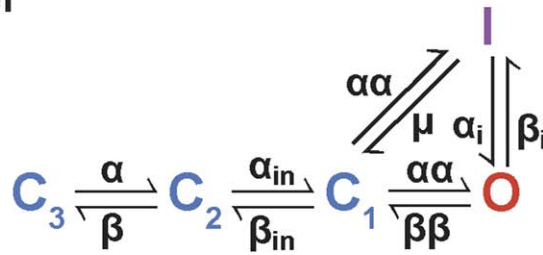
Repolarization of the cardiac action potential (AP) is a precisely controlled process, allowing adaptation of the AP duration to changes in heart rate. Tight control is achieved by a delicate dynamic balance between several inward and outward transmembrane currents. While this multiple-current mechanism is necessary for precise control and normal rate dependence of the AP, the delicate balance is easily perturbed by abnormal ion channel function and by interventions such as drugs. A major focus of the Cape Town Symposium was on hereditary arrhythmias and sudden death associated with abnormal repolarization. In recent years, major advances have been made in our understanding of the molecular processes that underlie mutation—induced alterations in ion channel function. However, ion channel function is studied in expression systems (e.g., in *Xenopus*

oocyte or HEK cells), removed from the physiological myocyte environment where channels participate in highly dynamic, nonlinear, and complex interactions to generate the AP. A challenge therefore remains to integrate the ion channels into the physiological system of the functioning cell. By doing so, a mechanistic link could be established between channel function (normal or altered by disease or drug) and functioning of the cell, organ, and whole organism. Genetically engineered animals (mostly transgenic mice) have been used to make genotype-phenotype mechanistic connections in the context of cardiac ion channel mutations and arrhythmia; we have developed and applied computational biology approaches to this problem.¹

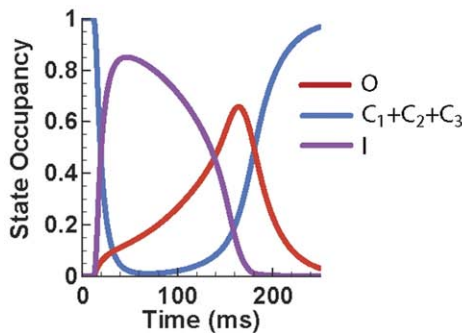
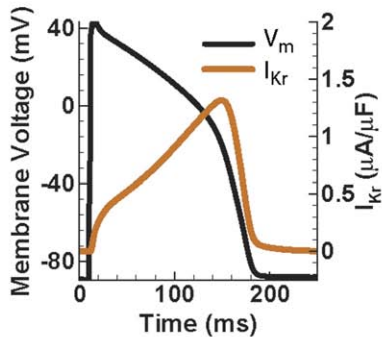
This article summarizes my two presentations at the Cape Town Symposium. The first part (first presentation) focuses on two major repolarizing currents I_{Kr} (rapid delayed rectifier) and I_{Ks} (slow delayed rectifier) carried by K^+ ions. Using computational biology, it provides mechanistic insights into how these channel gating processes determine their role in AP repolarization. The second, imaging part (second presentation) provides images of normal and abnormal repolarization of the intact human heart, which were obtained using a noninvasive electrocardiographic imaging modality (ECGI). The material presented in this conference proceedings article has been pub-

Y. Rudy chairs the scientific advisory board and holds equity in CardioInsight Technologies (CIT). CIT does not support any research conducted by YR, including that presented here. Supported by National Institutes of Health/National Heart, Lung and Blood Institute Merit Award no. R37-HL-033343 and grant no. RO1-HL-49054. **Address reprint requests and correspondence:** Yoram Rudy, Ph.D., F.A.H.A., F.H.R.S., Fred Saigh Distinguished Professor, Washington University in St. Louis, 290 Whitaker Hall, Campus Box 1097, One Brookings Drive, St. Louis, Missouri 63130-4899. E-mail address: rudy@wustl.edu.

A. I_{Kr} Model



B. 40th AP at CL=1000 ms



C. 40th AP at CL=300 ms

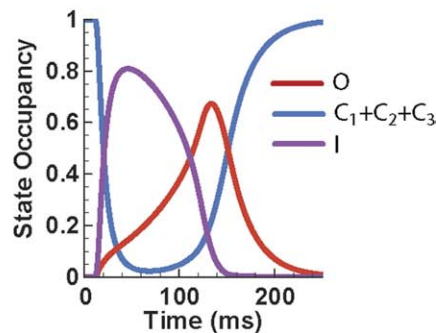
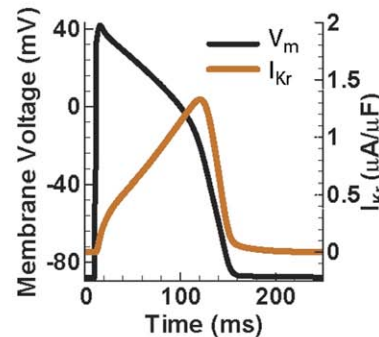


Figure 2 Kinetic transitions of I_{Kr} channels during the AP at slow and fast rate. **A:** Markov model of the I_{Kr} channel.²⁻⁴ States are color coded according to their type: closed (blue), inactivated (purple), open (red). **B:** I_{Kr} , V_m , and channel state occupancies during the 40th AP at slow rate, CL = 1000 ms. Even though I_{Kr} activates nearly instantaneously, few channels move into the open state because of rapid inactivation. Then, as V_m decreases, channels begin to recover from inactivation, generating a pronounced peak of open-state occupancy and peak current during the late phase of the AP. **C:** I_{Kr} , V_m , and channel state occupancies during the 40th AP at fast rate, CL = 300 ms. Surprisingly, peak I_{Kr} is not changed significantly at fast rate. Examination of the state occupancies (bottom panel) reveals that conditions at AP initiation are identical at fast and slow rates, preventing any current accumulation. However, faster increase of I_{Kr} at fast rate during the AP contributes to APD shortening. From reference 4 with permission.

Considering all possible combinations of the four voltage sensors' positions during gating, one obtains 15 closed states (C_1 – C_{15}) before channel opening. For example, C_1 represents all sensors in their R1 position; in C_4 , one sensor is in R1 and three in R2; in C_{11} , one is in R1, one in R2, and two in A. In C_{15} , all four voltage sensors are in the A position. Figure 3 shows the 15 closed states; horizontal (left to right) transitions represent movement of voltage sensors from position R1 to R2; vertical (top-down) transitions represent movement from R2 to A. The R1 to R2 transitions occur first and are relatively slow (transition rate $\alpha = 4.4S^{-1}$). The second transitions from R2 to A are an order of magnitude faster, with a transition rate $\alpha = 44.7S^{-1}$. Channels in closed states C_5 , C_9 , C_{12} , and C_{14} in the right column of the state diagram only need to undergo a fast transition from R2 to A before channel opening. Therefore, in the corre-

sponding Markov model of I_{Ks} kinetics (Figure 4A), closed states can be divided into two zones: zone 2 (green states) of channels with at least one voltage sensor in R1, requiring a first slow transition to R2 before the channel can open; and zone 1 (blue states) of channels that have completed all slow transitions into R1 and require only fast transitions from R1 to A before channel opening. Thus, channels in zone 2 are in deeper closed states that are kinetically remote from the open state, while channels in zone 1 are available to open rapidly. As will be shown, this partition into two classes of closed states with different kinetic properties underlies I_{Ks} participation in rate dependence of AP repolarization. I_{Ks} and its channel state occupancies during the AP are shown for slow rate (CL = 1000 ms) and fast rate (CL = 300 ms) in Figure 4B and 4C, respectively. At slow rate, 60% of channels reside in zone 2 at the onset of AP depolarization

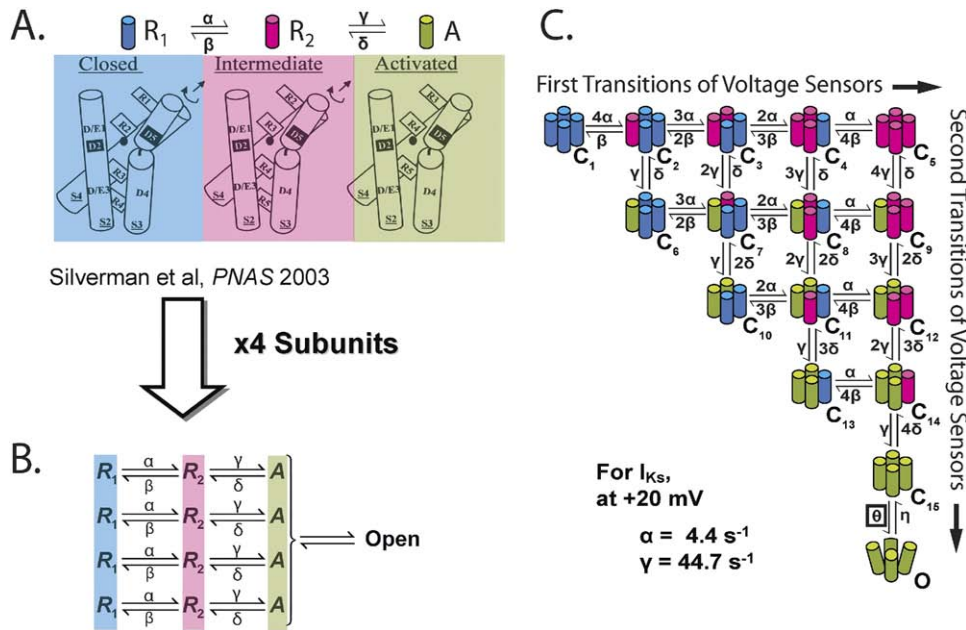


Figure 3 Conformational changes of K^+ channels during activation. **A:** Structural basis for two voltage sensor transitions before channel opening (modified from reference 10 with permission). **B:** Kinetic representation of the two voltage sensor transitions in panel A; all four α -subunits that form the channel undergo a first transition from a resting state (R_1) to an intermediate state (R_2) and a second transition from R_2 to an activated state (A). Once all voltage sensors are in the activated state, the channel can open. **C:** The total number of combinations of voltage sensor positions in the four subunits is 15 and can be represented by 15 closed states before channel opening. Blue, red, and green indicate a voltage sensor in position R_1 , R_2 or A , respectively (from reference 4 with permission). Panel A is based on data from ether-à-go-go (eag) and Shaker K^+ channels and is adapted from reference 10 with permission.

(panel B, bottom) and must undergo a slow transition to zone 1 before channel opening. At this rate, only 40% of the channels reside in zone 1, ready to open. At fast rate (panel C, bottom), 75% of channels accumulate in zone 1 before the AP upstroke, as they do not have sufficient time between APs to transition to zone 2. Thus, at fast rate an “available reserve” of channels is created in zone 1, facilitating fast channel openings and rapid rise of I_{Ks} current to a larger peak during the AP repolarization phase. This ability to generate a large current late during the AP plateau makes I_{Ks} an effective repolarizing current and determinant of APD and its rate dependence.

Noninvasive images of cardiac repolarization in humans

ECGI has been used for mapping normal and abnormal activation of the human heart *in vivo*. The ECGI procedure is shown in the diagram of Figure 5 (see references 5 and 6 for details). Here we provide examples of its application during repolarization, an application that was validated in animal experiments in which dispersion of repolarization was induced by local epicardial cooling and warming.¹³ Figure 6A shows noninvasively imaged epicardial potentials at peak T-wave from a normal subject. Two reconstructed epicardial electrograms from locations 1 (right ventricle) and 2 (left ventricle) are shown in panel B. The potential pattern of Figure 6A does not change much during the entire T wave, although potential magnitudes change substantially. The static pattern reflects the relatively slow repolarization process that encompasses the entire ventric-

ular myocardium. This is in contrast to the very dynamic activation process that involves propagation of excitation wave fronts. From the electrograms, activation times and recovery times at various epicardial locations can be determined. In the electrograms of Figure 6B, these times are marked by vertical lines. The local activation-recovery interval (ARI) is the difference between the recovery and activation times; it reflects the local APD.¹⁴ At location 1, ARI = 225 ms, and at location 2, ARI = 265 ms. These values are typical of the APD recorded in human ventricular myocytes; they indicate a longer APD in the left ventricle than in the right ventricle, with a 40-ms difference between the epicardial locations shown.

Figure 7 shows ECGI-imaged epicardial isochrones from a patient with Wolff-Parkinson-White (WPW) syndrome.⁷ Isochrones (activation sequences) are shown before ablation of the accessory pathway (left panel) and 45 minutes postablation (right panel). Before ablation, there is an area of early pre-excitation from the accessory pathway at the base (red; earliest site is marked with an asterisk). After ablation, the activation sequence is reversed with this region activating last (blue). Note that the T wave is negative preablation and remains so after ablation, indicating the presence of “cardiac memory.”^{15,16}

Figure 8 shows ARI maps preablation and at progressive times (45 minutes, 1 week, 1 month) postablation. Epicardial electrograms from the preexcitation area are also included. While the QRS reverses from negative to positive immediately after ablation, the T wave remains negative 45

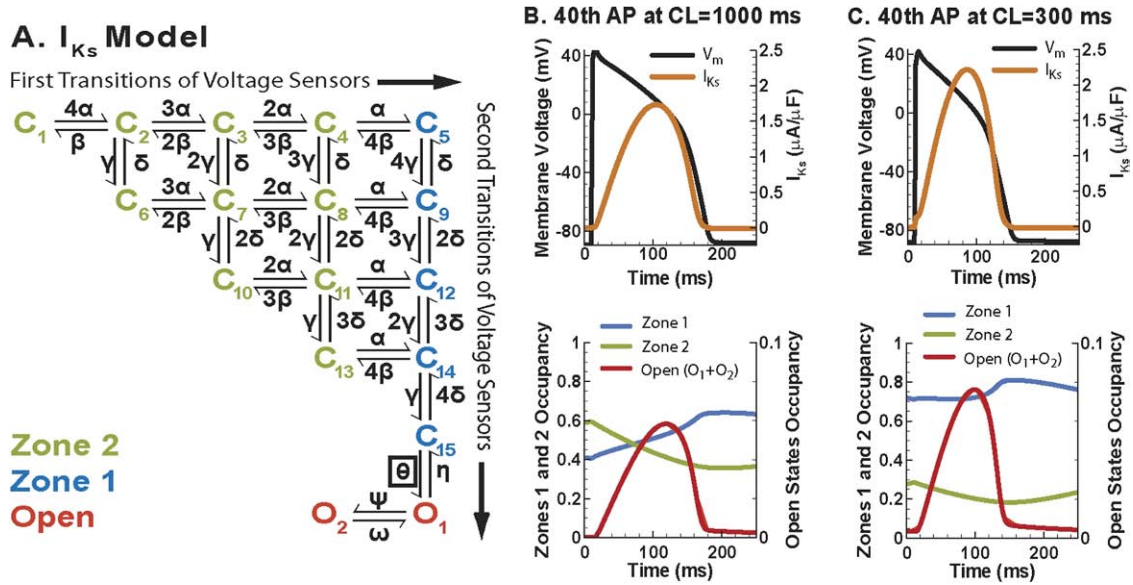


Figure 4 Kinetic transitions of I_{Ks} channels during the AP at slow and fast rate. **A:** Markov model of the I_{Ks} channel.³ States are color coded according to their type: zone 2, closed states for which not all voltage sensors have completed the first transition (light green); zone 1, closed states for which all four voltage sensors have completed the first transition (blue); open (red). **B:** I_{Ks} , V_m , and channel state occupancies during the 40th AP at slow rate, CL = 1000 ms. I_{Ks} rises slowly, resulting in peak current at the end of the AP, where it most efficiently contributes to repolarization. Only 40% of channels reside in zone 1 at AP onset and can activate rapidly. While V_m remains depolarized, channels continue to transition from zone 2 to zone 1. **C:** I_{Ks} , V_m , and channel state occupancies during the 40th AP at fast rate, CL = 300 ms. Since the diastolic interval is shorter at CL = 300 ms, V_m stays at depolarized potentials for a larger percentage of time, which causes accumulation in zone 1 of closed states. At AP onset, 75% of channels reside in zone 1, facilitating rapid transitions to the open state. This results in increased I_{Ks} late during the AP and APD shortening. Note that the mechanism for I_{Ks} increase is accumulation in closed states near the open state (zone 1) as opposed to open-state accumulation. The accumulation in zone 1 creates a reserve of channels that are ready to open rapidly, “on demand” to generate a greater repolarizing current; we call this pool of channels “available reserve.” From reference 4 with permission.

minutes and 1 week after ablation, becoming positive at 1 month postablation. ARIs from the preexcitation region are 350 ms, greatly prolonged compared with 300 ms during

normal sinus rhythm. Apical ARI is 240 ms, the same as normal, and the apex-to-base ARI gradient is 110 ms before the ablation procedure. This gradient remains unchanged 45

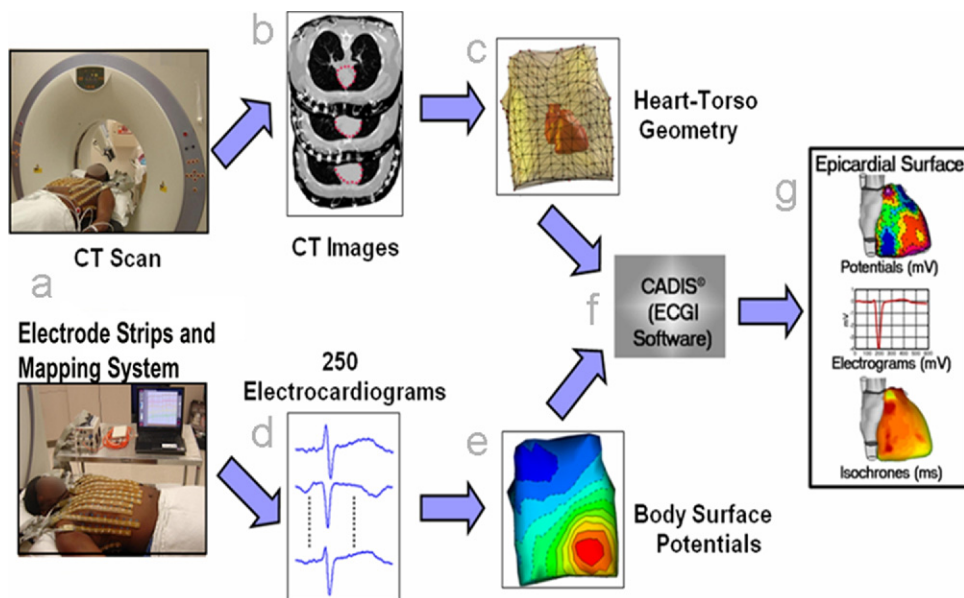


Figure 5 Block diagram of the ECGI procedure. (a) Multi-electrode (224 or 256) mapping system is used to obtain ECGs over the entire torso surface (bottom). CT scan, conducted during application of the electrodes, provides the heart-torso geometrical relationship (top). (b) Transverse CT slices showing the epicardial contour (red) and torso electrodes (shiny dots). (c) Three-dimensional heart-torso geometry constructed from the CT slices. (d) Sample ECG signals from the mapping system. (e) Body surface potential map obtained from the ECGs in panel d for one instance during the cardiac cycle. (f) ECGI software package reconstructs epicardial data from the data in panels c and e. (g) Examples of noninvasive ECGI images, including (top to bottom) epicardial potentials, electrograms, and isochrones. Adapted from reference 5.

Ventricular Repolarization

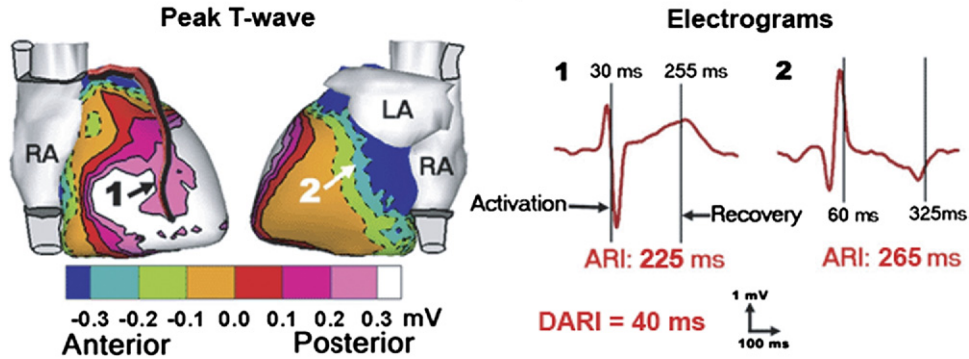


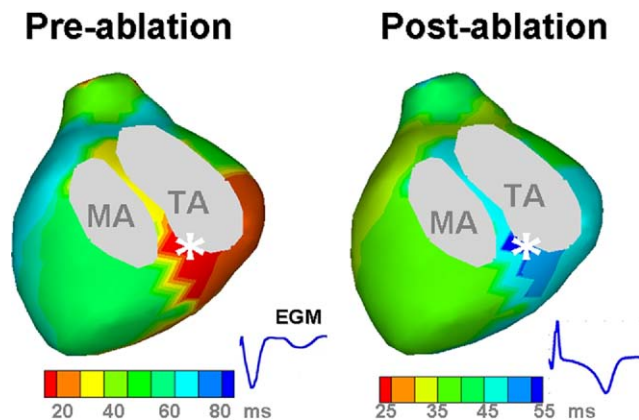
Figure 6 Noninvasive ECGI images of normal ventricular repolarization. *Left*, Epicardial potentials. Numbers indicate locations of electrograms shown on the right. *Right*, Examples of ECGI reconstructed electrograms on right ventricle (1) and left ventricle (2) epicardium. Vertical lines mark activation and recovery times. DARI, difference in ARI between locations 2 and 1. From reference 5.

minutes after ablation. It decreases to 80 ms at 1 week and to a normal value of 40 ms at 1 month. Thus, despite the immediate change of activation after ablation, abnormal repolarization persists and gradually returns to normal over a period of 1 month, exhibiting long-term memory.

Discussion

The cardiac AP is generated by complex, nonlinear interactions among ion channels, the membrane potential, the dynamic ionic environment of the cell, and various regulatory processes. Computational biology is a powerful tool for analyzing such complex interactions and for providing insights into mechanisms.¹⁷ The simulations presented here focus on the two major repolarizing currents, I_{Kr} and I_{Ks} . To play an effective role in cardiac AP repolarization, these currents need to gradually increase during the plateau, reaching a maximum at the late phase of the AP. As the simulations show, the two currents do so via very different mechanisms. I_{Kr} inactivates almost instantaneously after fast activation during the AP early phase. It then gradually recovers from inactivation during the plateau to reach a peak of open-channel occupancy and maximum current at

the late plateau phase. Thus I_{Kr} relies on gradual recovery during the AP to achieve maximum current when it most effectively affects AP repolarization. I_{Ks} relies on a two-stage voltage sensor movement to achieve a late peak current. At fast rate, channels accumulate between beats at zone 1 of closed states, building an available reserve of channels that can open during the AP to increase current at the late plateau phase. Conserving current for the late phase of the AP is crucial for effective participation of I_{Kr} and I_{Ks} in repolarization. Indeed, as we have shown in previous simulations,² mutations in I_{Kr} that prevent formation of the late peak of open channel occupancy result in major APD prolongation and the long QT syndrome. Also, if I_{Ks} buildup of an available reserve is eliminated, it cannot provide sufficient late current (“repolarization reserve”)¹⁸ to ensure AP repolarization without generation of arrhythmogenic early afterdepolarization when I_{Kr} is compromised by mutations or drugs.³



Figures 7 ECGI-imaged epicardial activation maps in a WPW patient. *Left*, Preablation. *Right*, Postablation. Electrogram (EGM) from the preexcitation region is also shown. Adapted from reference 7 with permission.

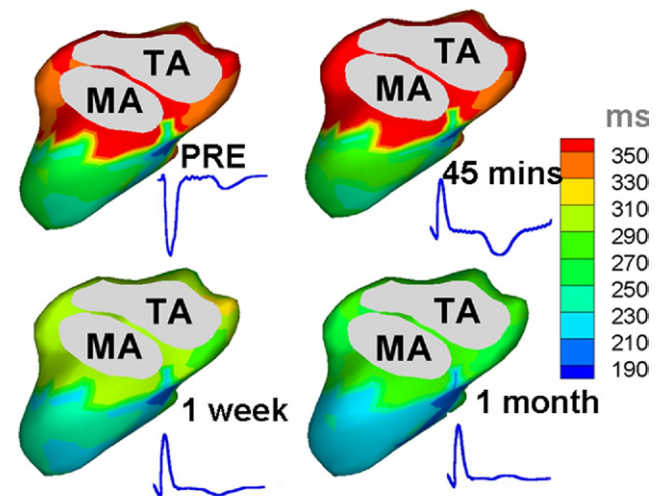


Figure 8 Epicardial ARI maps preablation and at different times (45 minutes, 1 week, and 1 month) postablation. EGM from preexcitation region is also shown. MA = mitral annulus; TA = tricuspid annulus. Adapted from reference 7 with permission.

The last section of the paper demonstrates the ability of ECGI to image noninvasively repolarization of the human heart. Abnormally steep spatial gradients of repolarization (“repolarization dispersion”) provide a substrate for development of unidirectional block and reentrant arrhythmias. The images show a normal right and left ventricle repolarization gradient of 40 ms; a similar gradient exists from apex to base in the normal heart.⁶ Preexcitation associated with WPW prolongs repolarization in the preexcitation region, increasing greatly the apex-base dispersion to 110 ms.⁷ After ablation of the accessory pathway, this gradient persists and gradually becomes normal (40 ms) over a period of 1 month. The persistence of abnormal repolarization is indicative of long-term cardiac memory; the 1-month time course of its dissipation is consistent with transcriptional reprogramming and remodeling of ion channels.¹⁵

Acknowledgment

The author thanks Kimberly Smith for her help in preparing the manuscript.

References

1. Clancy CE, Rudy Y. Linking a genetic defect to its cellular phenotype in a cardiac arrhythmia. *Nature* 1999;400:566–569.
2. Clancy CE, Rudy Y. Cellular consequences of HERG mutations in the long QT syndrome: precursors to sudden cardiac death. *Cardiovasc Res* 2001;50:301–313.
3. Silva J, Rudy Y. Subunit interaction determines IKs participation in cardiac repolarization and repolarization reserve. *Circulation* 2005;112:1384–1391.
4. Rudy Y, Silva J. Computational biology in the study of cardiac ion channels and cell electrophysiology. *Q Rev Biophys* 2006;39:57–116.
5. Ramanathan C, Ghanem RN, Jia P, et al. Noninvasive electrocardiographic imaging for cardiac electrophysiology and arrhythmia. *Nat Med* 2004;10:422–428.
6. Ramanathan C, Jia P, Ghanem RN, et al. Activation and repolarization of the normal human heart under complete physiological conditions. *Proc Natl Acad Sci U S A* 2006;103:6309–6314.
7. Ghosh S, Rhee E, Avari J, et al. Cardiac memory in patients with Wolff-Parkinson-White syndrome: noninvasive imaging of activation and repolarization before and after catheter ablation. *Circulation* 2008;108:907–915.
8. Chen H, Kim LA, Rajan S, et al. Charybdotoxin binding in the I(Ks) pore demonstrates two MinK subunits in each channel complex. *Neuron* 2003;40:15–23.
9. Zagotta WN, Hoshi T, Dittman J, et al. Shaker potassium channel gating. II. Transitions in the activation pathway. *J Gen Physiol* 1994;103:279–319.
10. Silverman WR, Roux B, Papazian DM. Structural basis of two-stage voltage-dependent activation in K⁺ channel. *Proc Natl Acad Sci U S A* 2003;100:2935–2940.
11. Koren G, Liman ER, Logothetis DE, et al. Gating mechanism of a cloned potassium channel expressed in frog oocytes and mammalian cells. *Neuron* 1990;4:39–51.
12. Nekouzadeh A, Silva JR, Rudy Y. Modeling subunit cooperativity in opening of tetrameric ion channels. *Biophys J* 2008;95:3510–3520.
13. Ghanem RN, Burnes JE, Waldo AL, et al. Imaging dispersion of myocardial repolarization. II. Noninvasive reconstruction of epicardial measures. *Circulation* 2001;104:1306–1312.
14. Haws CW, Lux RL. Correlation between in vivo transmembrane action potential durations and activation-recovery intervals from electrograms: effects of interventions that alter repolarization time. *Circulation* 1990;81:281–288.
15. Rosen MR, Cohen I. Cardiac memory: new insights into molecular mechanisms. *J Physiol* 2005;570:209–218.
16. Rosenbaum MB, Blanco HH, Elizari MV, et al. Electronic modulation of the T wave and cardiac memory. *Am J Cardiol* 1982;50:213–222.
17. Rudy Y, Ackerman MJ, Bers DM, et al. Systems approach to understanding electromechanical activity in the human heart. A national Heart, Lung, and Blood Institute Workshop summary. *Circulation* 2008;118:1202–1211.
18. Roden DM. Drug-induced prolongation of the QT interval. *N Eng J Med* 2004;350:1013–1022.